Photoinduced Electron and Energy Transfer in Molecular Pentads

Devens Gust,* Thomas A. Moore,* Ana L. Moore,* Alisdair N. Macpherson, Arnaldo Lopez, Janice M. DeGraziano, Isabelle Gouni, Edith Bittersmann, Gilbert R. Seely, Feng Gao, Ronald A. Nieman, Xiaochun C. Ma, Lori J. Demanche, Su-Chun Hung, David K. Luttrull, Seung-Joo Lee, and Pamela K. Kerrigan

Contribution from the Department of Chemistry and Biochemistry, Center for the Study of Early Events in Photosynthesis, Arizona State University, Tempe, Arizona 85287-1604

Received May 27, 1993®

Abstract: A series of molecular pentads, each consisting of a porphyrin dyad (P-P) covalently linked to a carotenoid polyene (C) and a diquinone moiety (Q_A-Q_B), have been prepared, and the photochemical properties of these molecules have been studied using steady-state and transient absorption and emission spectroscopies. Each of the pentads undergoes photoinduced electron transfer from the C-P-^{1}P-Q_A-Q_B singlet state to yield the charge-separated state C-P-P$^{\bullet+}$-$Q_A^{\bullet-}$-Q_B. Competing with charge recombination of this species are additional electron-transfer reactions operating in series and in parallel which converge on a final C$^{\bullet+}$-P-P-Q_A-$Q_B^{\bullet-}$ state. The electron-transfer rate constants and the quantum yields of the various charge-separated species are sensitive functions of the state energies and the electronic coupling between the porphyrin and diquinone moieties. One of the pentads undergoes photoinduced electron transfer to produce the final C$^{\bullet+}$-P-P-Q_A-$Q_B^{\bullet-}$ state with a quantum yield of 0.83 and a lifetime of 55 μs. This example of an artificial photosynthetic reaction center preserves about half of the initial excited singlet state energy as chemical potential. Other pentads have charge-separation lifetimes of several hundred microseconds.

Introduction

Photosynthetic reaction centers, which are responsible for the conversion of light energy into chemical potential in plants and other photosynthetic organisms, employ a variety of photoinduced electron and energy transfer processes in order to achieve their purpose. These events occur among organic pigments and other cofactors that are embedded in and organized by a protein matrix. One approach to artificial photosynthesis, or mimicry of the natural process, is to employ cofactors related to those found in reaction centers, but to use covalent linkages, rather than protein, as an organizing principle.[1-8] One of the more remarkable features of natural reaction centers is their ability to use excitation energy to quickly separate charge with high quantum yield over large distances while retarding energy-wasting charge recombination to the ground state. This is achieved at least in part by a multistep electron-transfer sequence. Charge is separated by a series of short-range, fast, and efficient electron-transfer steps to yield a final charge-separated state that is long-lived because the negative and positive charges are spatially and electronically well isolated.

Some time ago,[9,10] we reported the synthesis and study of a covalently linked carotenoid (C) porphyrin (P) quinone (Q) triad molecule that mimicked this multistep electron-transfer strategy. Excitation of the porphyrin moiety yields the first excited singlet state C-^{1}P-Q, which donates an electron to the quinone to give an intermediate C-P$^{\bullet+}$-Q$^{\bullet-}$ charge-separated state. Competing with recombination of this state is electron transfer from the carotenoid secondary donor to the porphyrin to yield a final C$^{\bullet+}$-P-Q$^{\bullet-}$ species that lives at least 10 000 times longer than the P$^{\bullet+}$-Q$^{\bullet-}$ states formed following excitation of related porphyrin–quinone dyads. The successful implementation of the multistep electron-transfer strategy in this simple triad has led to the preparation and study of a variety of more complex multicomponent molecular species which, by virtue of this complexity, are able to demonstrate a variety of multistep transfer phenomena precluded in simpler systems.[1-8] Herein we report the synthesis and spectroscopic study of carotenoid–diporphyrin–diquinone pentads **1–5** (Chart I), which employ a variety of sequential and parallel multistep electron-transfer strategies to produce long-lived charge-separated states, often in high quantum yield.[11,12]

Results

The synthesis and characterization of **1–5** and related model compounds are described in detail in the supplementary material. In order to understand the sometimes complex photochemistry of the pentads, it is appropriate to consider first some simpler compounds. We will begin by briefly recapitulating the previously reported results for diporphyrin **6** (Chart II).[13]

Dyad 6. This molecule consists of two very similar tetraarylporphyrin moieties joined by an amide linkage. Both ^{1}H NMR studies and molecular mechanics calculations show that the partial double bond character of the amide restricts the molecule to extended conformations in which the porphyrins are directed out, away from one another, rather than folded arrangements. Thus, the interporphyrin separation (~19 Å

* Abstract published in *Advance ACS Abstracts*, November 1, 1993.

(1) Gust, D.; Moore, T. A. *Science* **1989**, *244*, 35–41.
(2) Gust, D.; Moore, T. A. *Adv. Photochem.* **1991**, *16*, 1–65.
(3) Gust, D.; Moore, T. A. *Top. Curr. Chem.* **1991**, *159*, 103–151.
(4) Gust, D.; Moore, T. A.; Moore, A. L. *Acc. Chem. Res.* **1993**, *26*, 198–205.
(5) Connolly, J. S.; Bolton, J. R. In *Photoinduced Electron Transfer*; Fox, M. A., Channon, M., Eds.; Elsevier: Amsterdam, 1988; Part D, pp 303–393.
(6) Wasielewski, M. R. *Chem. Rev.* **1992**, *92*, 435–461.
(7) Bixon, M.; Fajer, J.; Feher, G.; Freed, J. H.; Gamliel, D.; Hoff, A. J.; Levanon, H.; Mobius, K.; Nechushtai, R.; Norris, J. R.; Scherz, A.; Sessler, J. L.; Stehlik, D. *Isr. J. Chem.* **1992**, *32*, 449–455.
(8) Asahi, T.; Ohkohchi, M.; Matsusaka, R.; Mataga, N.; Zhang, R. P.; Osuka, A.; Maruyama, K. *J. Am. Chem. Soc.* **1993**, *115*, 5665–5674.
(9) Gust, D.; Mathis, P.; Moore, A. L.; Liddell, P. A.; Nemeth, G. A.; Lehman, W. R.; Moore, T. A.; Bensasson, R. V.; Land, E. J.; Chachaty, C. *Photochem. Photobiol.* **1983**, *37S*, S46.
(10) Moore, T. A.; Gust, D.; Mathis, P.; Mialocq, J.-C.; Chachaty, C.; Bensasson, R. V.; Land, E. J.; Doizi, D.; Liddell, P. A.; Lehman, W. R.; Nemeth, G. A.; Moore, A. L. *Nature (London)* **1984**, *307*, 630–632.
(11) Some of the results for **1** and **2** have appeared in preliminary form.[12]
(12) Gust, D.; Moore, T. A.; Moore, A. L.; Lee, S.-J.; Bittersmann, E.; Luttrull, D. K.; Rehms, A. A.; DeGraziano, J. M.; Ma, X. C.; Gao, F.; Belford, R. E.; Trier, T. T. *Science* **1990**, *248*, 199–201.
(13) Gust, D.; Moore, T. A.; Moore, A. L.; Gao, F.; Luttrull, D.; DeGraziano, J. M.; Ma, X. C.; Makings, L. R.; Lee, S.-J.; Trier, T. T.; Bittersmann, E.; Seely, G. R.; Woodward, S.; Bensasson, R. V.; Rougée, M.; De Schryver, F. C.; Van der Auweraer, M. *J. Am. Chem. Soc.* **1991**, *113*, 3638–3649.

0002-7863/93/1515-11141$04.00/0

Chart I

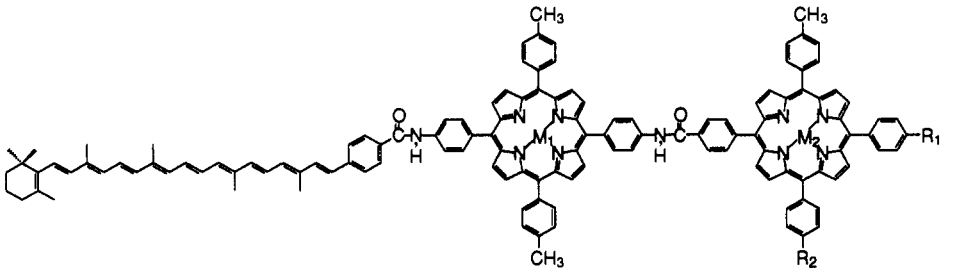

1: $M_1 = H_2$, $M_2 = H_2$, $R_2 = CH_3$, $R_1 =$ 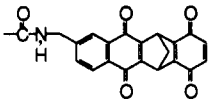

2: $M_1 = Zn$, $M_2 = H_2$, $R_2 = CH_3$, $R_1 =$ 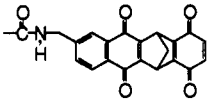

3: $M_1 = Zn$, $M_2 = Zn$, $R_2 = CH_3$, $R_1 =$ 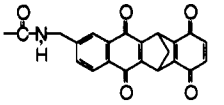

4: $M_1 = Zn$, $M_2 = H_2$, $R_2 = CH_3$, $R_1 =$ 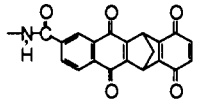

5: $M_1 = Zn$, $M_2 = H_2$, $R_1 = CH_3$, $R_2 =$ 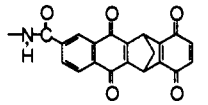

Chart II

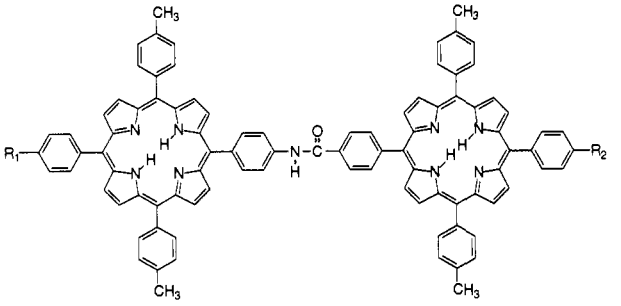

6: $R_1 =$ 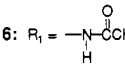 , $R_2 =$ 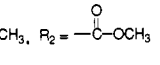

9: $R_1 = -NH_2$, $R_2 =$ 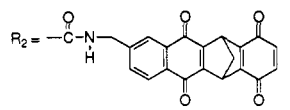

Chart III

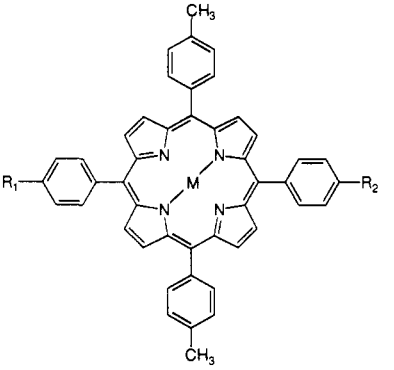

7: $R_1 = R_2 =$ 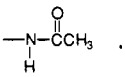 , $M = H_2$

8: $R_1 = R_2 =$ 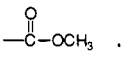 , $M = H_2$

14: $R_1 = -NH_2$ $R_2 = -CH_3$, $M = Zn$

center-to-center) is well-defined, although the interporphyrin dihedral angles are not known with certainty. The absorption spectrum of **6** in dichloromethane solution features maxima at 422, 518, 554, 594, and 650 nm and is virtually identical with a linear combination of the spectra of model porphyrin monomers **7** and **8** (Chart III). Linking the moieties does not significantly perturb the ground or excited singlet states of the individual chromophores.

The corrected fluorescence emission spectrum of **6** in dichloromethane is similar to those of **7** and **8**, with maxima at 655 and 720 nm. The lifetime of the excited singlet states following excitation at 590 nm, as measured by observation of the fluorescence decay by the single-photon timing technique, is 7.8 ns, which is virtually identical to those of models **7** (7.9 ns) and **8** (8.3 ns). Thus, linking the chromophores has not introduced any new pathways for quenching of the first excited singlet states.

In particular, photoinduced electron transfer to yield a $P^{\bullet+}$-$P^{\bullet-}$ charge-separated state does not occur due to unfavorable thermodynamics.[13] The energy of the porphyrin excited singlet states (as calculated from the average of the frequencies of the longest-wavelength absorption maxima and shortest-wavelength emission maxima) is 1.90 eV, whereas the lowest-energy charge-separated state lies about 2.11 eV above the ground state (as estimated from the first oxidation and first reduction potentials of model compounds determined by cyclic voltammetry). Thus, photoinduced electron transfer is endergonic and cannot compete with the usual deactivation pathways. In this and other estimates in this report, no corrections for Coulombic stabilization of charge-separated states have been made.

Chart IV

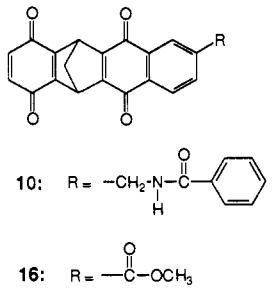

Scheme I

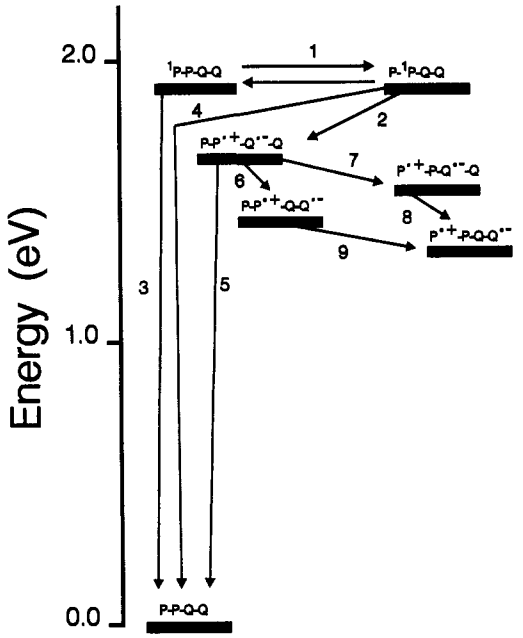

Tetrad 9. With these results in mind, we turn to P-P-Q_A-Q_B tetrad **9**, which consists of a diporphyrin moiety similar to **6** bearing a diquinone electron acceptor. The diquinone features a naphthoquinone group linked to a benzoquinone via a rigid, bicyclic bridge. This rigidity, coupled with that of the amide linkage, prevents the molecule from folding back on itself and "short-circuiting" the electron-transfer processes to be described below.

The visible absorption spectrum of **9** in dichloromethane is identical to that of dyad **6**, within experimental error, as is the fluorescence emission spectrum. The fluorescence decay profiles following excitation of **9** with a 590-nm laser pulse were measured at six wavelengths in the 650–740-nm region. The decays were analyzed globally[14] as a single-exponential process with a lifetime of 4.5 ns ($\chi^2 = 1.07$). The short lifetime relative to those for **6–8** indicates that the porphyrin first excited singlet states are being quenched. The quenching is ascribed to electron transfer from P-^{1}P-Q_A-Q_B to the naphthoquinone to yield the P-P$^{\bullet+}$-$Q_A^{\bullet-}$-Q_B charge-separated state (step 2 in Scheme I). Cyclic voltammetric studies of model diquinone **10** (Chart IV) in 1,2-dichloroethane (see experimental section) yielded reversible voltammograms with first and second reduction potentials of –0.85 and –1.07 V relative to a ferrocene internal reference redox system. These results, coupled with previously reported redox potentials for model porphyrins,[13] yield the energetics shown in Scheme I. The electron-transfer step 2 is exergonic by ~0.25 eV. Results from related porphyrin–quinone[1-8] and porphyrin–diquinone systems[15,16] and from the pentads to be discussed below are consistent with this interpretation. In addition, time-resolved transient absorption studies of an amide-linked porphyrin–quinone dyad and carotenoid–porphyrin–quinone triad have demonstrated that the rate of decay of the porphyrin first excited singlet state, as measured by time-resolved fluorescence spectroscopy, and the rate of appearance of the charge-separated state are identical.[17]

Given the electron transfer by step 2 in Scheme I, one might expect to observe two components in the fluorescence decay of **9**, one with a long lifetime due to ^{1}P-P-Q_A-Q_B and a second, shorter-lived component from P-^{1}P-Q_A-Q_B. The observation of a single lifetime implies that the two porphyrin moieties exchange excitation energy via singlet–singlet energy transfer, which is rapid on the time scale of porphyrin singlet decay (step 1 in Scheme I and its reverse). Such transfer has been observed in closely related porphyrin dyads,[13] but is not detected directly in this case because the two porphyrin moieties have virtually identical absorption and emission spectra. This being the case, the two porphyrin first excited singlet states of **9** will have identical lifetimes, τ_f, given by eq 1. Values for k_3 and k_4 of 1.3×10^8 and

$$1/\tau_f = (k_2 + k_3 + k_4)/2 \qquad (1)$$

1.2×10^8 s^{-1} may be estimated from the fluorescence lifetimes of **7** and **8** given above, and τ_f is 4.5 ns. Thus, the photoinduced electron-transfer rate constant k_2 equals 1.9×10^8 s^{-1} (Table I). The quantum yield of electron transfer based upon the total light absorbed by the two porphyrins, determined from eq 2, equals 0.43.

$$\Phi_2 = k_2/(k_2 + k_3 + k_4) \qquad (2)$$

Given the formation of P-P$^{\bullet+}$-$Q_A^{\bullet-}$-Q_B in **9**, it is clear that, from a thermodynamic point of view (Scheme I), the charge-separated state could either recombine by step 5 or undergo additional electron-transfer steps to yield new charge-separated species. The latter possibility has been investigated through the synthesis and study of the pentad molecules.

Pentad 1. Pentad **1** was prepared from tetrad **9** by linking a synthetic carotenoid to the amino group. The conformation of the molecule is extended, as shown in Figure 1, which is derived from molecular mechanics calculations performed using the CHARMm program in the QUANTA molecular-modeling package from Polygen Corp. The calculations involved defining the force field for the pentad components followed by energy minimization. The force field was assigned by the choice of suitable atom-type parameters that combine to define the force constants for the various bonds and other interactions. For most of the atoms, the usual CHARMm atom types were retained. However, it was necessary to increase the constants for torsion about the bonds in the porphyrin macrocycles in order to allow the program to minimize to a porphyrin structure similar to those observed by X-ray crystallography. The minimization procedure was an adopted basis Newton–Raphson method suitable for relatively large molecules. It proved necessary to minimize the energies of the porphyrin, carotenoid, and quinone moieties individually, and then to constrain these structures and allow the final minimization to occur only about the bonds in the linkages. The extended conformation shown in Figure 1, with an overall length of ~80 Å, is consistent with ^{1}H NMR results, which rule out folded conformations with concomitant shielding of hydrogen atoms by porphyrin aromatic ring currents.[18] A related conformation with a dihedral angle between the planes of the porphyrin macrocycles of ~90° was of about the same energy.

The absorption spectrum of **1** in dichloromethane is shown in Figure 2. It resembles that of **9**, with porphyrin Q-band

(14) Wendler, J.; Holzwarth, A. *Biophys. J.* **1987**, *52*, 717–728.
(15) Gust, D.; Moore, T. A.; Moore, A. L.; Barrett, D.; Harding, L. O.; Makings, L. R.; Liddell, P. A.; DeSchryver, F. C.; Van der Auweraer, M.; Bensasson, R. V.; Rougée, M. *J. Am. Chem. Soc.* **1988**, *110*, 321–323.
(16) Hasharoni, K.; Levanon, H.; Tang, J.; Bowman, M. K.; Norris, J. R.; Gust, D.; Moore, T. A.; Moore, A. L. *J. Am. Chem. Soc.* **1990**, *112*, 6477–6481.
(17) Hung, S.-C.; Lin, S.; Macpherson, A. N.; DeGraziano, J. M.; Kerrigan, P. K.; Liddell, P. A.; Moore, A. L.; Moore, T. A.; Gust, D. *J. Photochem. Photobiol.*, in press.
(18) Chachaty, C.; Gust, D.; Moore, T. A.; Nemeth, G. A.; Liddell, P. A.; Moore, A. L. *Org. Magn. Reson.* **1984**, *22*, 39–46.

Table I. Rate Constants, Lifetimes, and Quantum Yields for Energy- and Electron-Transfer Processes[a]

	$k_1 \times 10^{-8}$ (s^{-1})		$k_2 \times 10^{-8}$ (s^{-1})		$k_3 \times 10^{-8}$ (s^{-1})[b]		$k_4 \times 10^{-8}$ (s^{-1})[b]		τ_{fi} (μs)[c]		Φ_{fi}[d]	
compd	$CHCl_3$	CH_2Cl_2	$CHCl_3$	CH_2Cl_2	$CHCl_3$	CH_2Cl_2	$CHCl_3$	CH_2Cl_2	$CHCl_3$	CH_2Cl_2	$CHCl_3$	CH_2Cl_2
1				2.3		2.9		1.2		340		0.15[e]
2	230	250	7.1	2.9	27	32	1.3	1.2	55	200	0.83[f]	0.60[f]
3				48		32		6.8		120		0.15[e]
4	~230	~230	710	~710	27	32	1.4	1.2	5.3	64	0.28[f] 0.22[e]	0.04[e,f]
5	~230	~230	~710	~710	27	32	1.4	1.2	0.42	46	0.24[f] 0.18[e]	0.05[e,f]
9				1.9		1.3		1.2				
11					2.9	2.9						
12					27	32						
13	230		≪1		27		1.4					
15			590	550			1.3	1.2				

[a] The processes represented by these rate constants are identified in Scheme III using pentad **2** as an example. [b] Estimated for triads, tetrads, and pentads from rate constants for appropriate model systems (see text). [c] Lifetime of the final $C^{\bullet+}$-P-P-Q_A-$Q_B^{\bullet-}$ state (±20%). [d] Quantum yield of the final $C^{\bullet+}$-P-P-Q_A-$Q_B^{\bullet-}$ state (±30%). [e] With 590-nm excitation. [f] With 650-nm excitation.

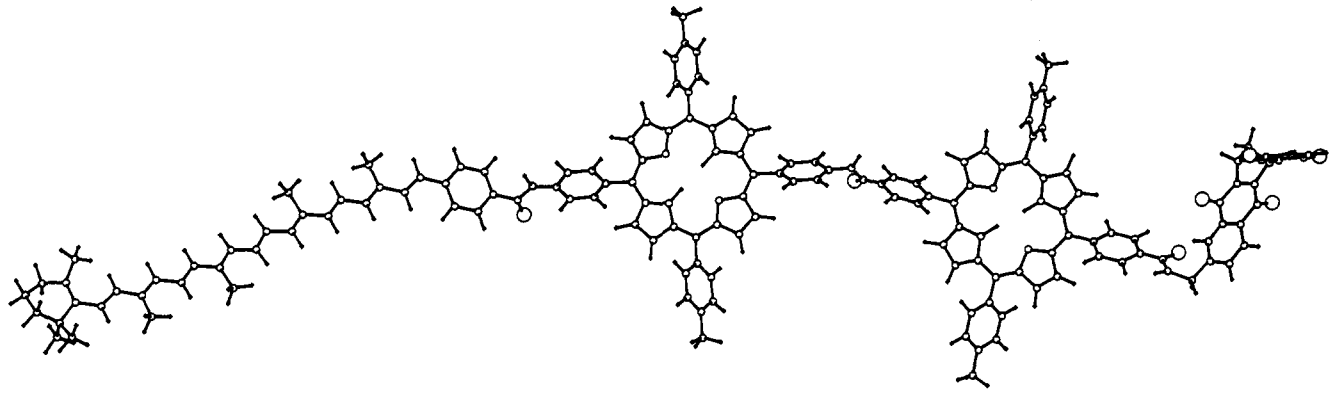

Figure 1. Conformation of pentad **1** as derived from molecular mechanics calculations. A related conformation with an angle of ~90° between the planes of the porphyin macrocycles was of approximately the same energy.

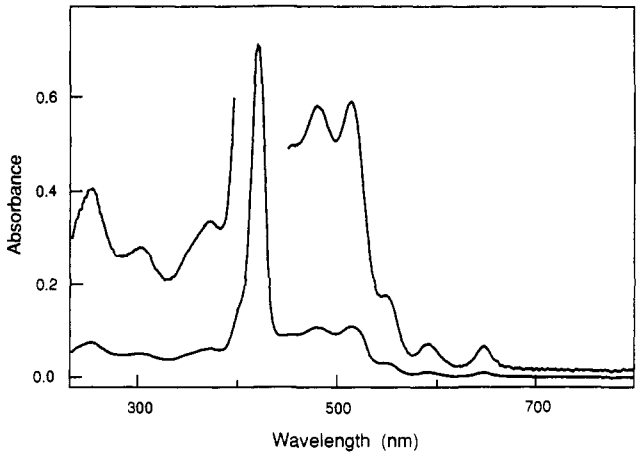

Figure 2. Absorption spectrum of pentad **1** in dichloromethane solution. The expansion (×5.5) has been offset from the base line for clarity.

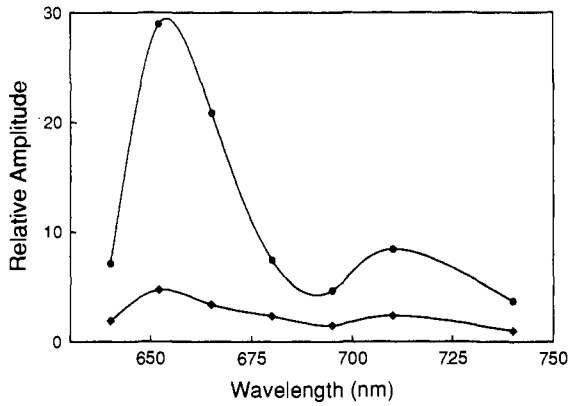

Figure 3. Decay-associated fluorescence emission spectrum for ca. 1 × 10^{-6} M free base pentad **1** in dichloromethane solution following excitation at 590 nm. The spectrum was obtained from a global analysis of data at the seven indicated wavelengths ($\chi^2 = 1.08$) analyzed as two exponentials with lifetimes of 3.13 (●) and 1.99 ns (◆).

absorptions at 650, 594, ~554, and ~518 nm, a Soret band at 422 nm, and quinone absorptions at <400 nm. Superimposed upon these bands is the carotenoid absorption, with maxima in the 450-520-nm region. As is the case with **6** and **9**, the absorption spectrum of **1** is essentially a linear combination of those of its component chromophores.

The shape of the fluorescence emission spectrum of **1** is identical to those of **6** and **9**, with maxima at 655 and 720 nm. Fluorescence decay measurements of **1** in dichloromethane were carried out with laser excitation at 590 nm. Decays were measured at seven wavelengths in the 640–740-nm region and analyzed globally. A satisfactory fit to all the data ($\chi^2 = 1.08$) was obtained using two exponential components with lifetimes of 3.13 and 1.99 ns (Figure 3). The minor component with the shorter lifetime likely represents an impurity, as its amplitude was dependent upon the degree of sample purification.

These results may be interpreted by reference to Scheme II, which shows the relevant transient states. Excitation at 590 nm yields an essentially equimolar mixture of C-P-^{1}P-Q_A-Q_B and C-^{1}P-P-Q_A-Q_B. These two species undergo rapid singlet–singlet energy transfer, as was observed for **6** and **9**, and decay via various photochemical processes (steps 3 and 4) and electron transfer by step 2 to yield C-P-$P^{\bullet+}$-$Q_A^{\bullet-}$-Q_B. The rate constant for step 3 may be estimated as 2.9×10^8 s^{-1} on the basis of 3.4-ns singlet lifetime of carotenoporphyrin **11** (Chart V) and related molecules,[19] whereas k_4 equals 1.2×10^8 s^{-1} as discussed above. This being the case, eq 1 yields a value for k_2 of 2.3×10^8 s^{-1}, which is very similar to the corresponding rate constant determined for

Chart V

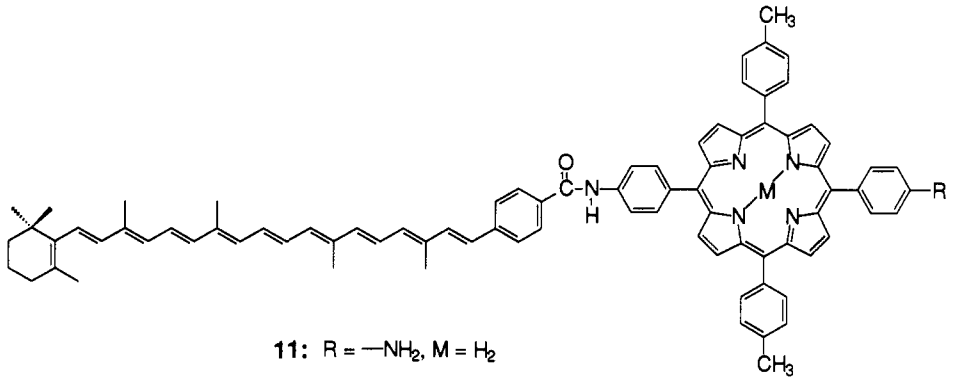

11: R = —NH_2, M = H_2

12: R = —N(H)—C(=O)CH_3, M = Zn

Scheme II

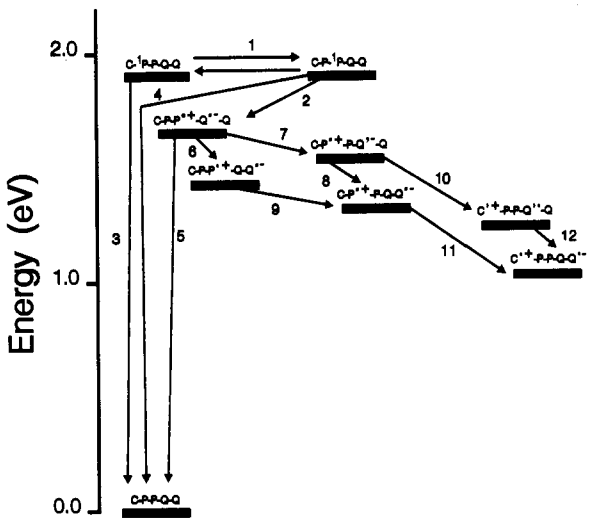

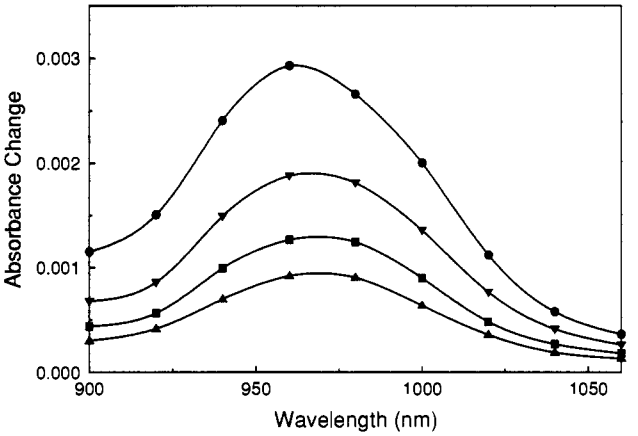

Figure 4. Transient absorbance following excitation of a solution of free base pentad **1** in dichloromethane with a 10-ns, 590-nm laser pulse. The broad absorption is that of the carotenoid radical cation of $C^{\bullet+}$-P-P-Q_A-$Q_B^{\bullet-}$ taken 32 (●), 192 (▼), 352 (■), and 512 μs (▲) after the excitation pulse.

9 (Table I). Thus, appending the carotenoid to tetrad **9** has essentially no effect upon the rate constant for photoinduced electron transfer to the diquinone. Equation 2 gives a quantum yield Φ_2 for the C-P-$P^{\bullet+}$-$Q_A^{\bullet-}$-Q_B charge-separated state of 0.36.

Scheme II suggests that although C-P-$P^{\bullet+}$-$Q_A^{\bullet-}$-Q_B undoubtedly decays rapidly by step 5, electron transfer via steps 6 and 7 could compete with charge recombination, beginning an electron-transfer cascade that would converge on final $C^{\bullet+}$-P-P-Q_A-$Q_B^{\bullet-}$ species. The final state might be expected to have a relatively long lifetime, as the positive and negative charges would be well separated. Transient absorption spectroscopy on the nanosecond time scale was used to investigate this possibility. Excitation of a dichloromethane solution of **1** with a 10-ns laser pulse at 590 nm resulted in the observation of a strong transient absorption with a maximum at ~960 nm (Figure 4). On the basis of results with model compounds,[20] this absorption can be assigned to the carotenoid radical cation of the $C^{\bullet+}$-P-P-Q_A-$Q_B^{\bullet-}$ charge-separated species. Thus, electron transfer occurs via at least some of the pathways 6–12 in Scheme II. The overall quantum yield of $C^{\bullet+}$-P-P-Q_A-$Q_B^{\bullet-}$ was estimated as 0.15 using the comparative method with the tetraphenylporphyrin triplet as a standard.[10,21]

The results in Figure 4 show that there is still a significant amount of charge-separated species present in solution even 0.5 ms after excitation. The decay of the transient at 960 nm could be fitted with an exponential lifetime of ~340 μs superimposed upon a small base-line offset due to a slowly decaying component. The 340-μs component is ascribed to the lifetime for intramolecular charge recombination of $C^{\bullet+}$-P-P-Q_A-$Q_B^{\bullet-}$. The amount of the minor, long-lived component varies with the concentration of the solution and likely represents, at least in part, the transfer of an electron between $C^{\bullet+}$-P-P-Q_A-$Q_B^{\bullet-}$ and a neutral ground-state molecule to generate individual radical cations and anions that decay slowly. The long lifetime and high energy of the $C^{\bullet+}$-P-P-Q_A-$Q_B^{\bullet-}$ state also make it susceptible to reaction with added or adventitious electron donors and acceptors present at very small concentrations.

These transient absorption results locate the radical cation on the carotenoid moiety, but do not specify which quinone is present as the radical anion. The energetics shown in Scheme II indicate that migration of the negative charge from the naphthoquinone Q_A to the benzoquinone Q_B is thermodynamically favored. Transient fluorescence, absorption, and electron paramagnetic resonance studies of a closely related C-P-Q_A-Q_B tetrad system unambiguously demonstrate that, in these compounds, the long-lived charge-separated state involves a carotenoid radical cation and a benzoquinone radical anion.[15,16]

Pentad 2. The quantum yield data for **1** show that a major loss of quantum efficiency in this molecule results from inefficient competition of the secondary or "dark" electron-transfer reactions

(19) Gust, D.; Moore, T. A.; Liddell, P. A.; Nemeth, G. A.; Makings, L. R.; Moore, A. L.; Barrett, D.; Pessiki, P. J.; Bensasson, R. V.; Rougée, M.; Chachaty, C.; De Schryver, F. C.; Van der Auweraer, M.; Holzwarth, A. R.; Connolly, J. S. *J. Am. Chem. Soc.* **1987**, *109*, 846–856.

(20) Land, E. J.; Lexa, D.; Bensasson, R. V.; Gust, D.; Moore, T. A.; Moore, A. L.; Liddell, P. A.; Nemeth, G. A. *J. Phys. Chem.* **1987**, *91*, 4831–4835.

(21) Bensasson, R. V.; Land, E. J.; Truscott, T. G. *Flash Photolysis and Pulse Radiolysis. Contributions to the Chemistry of Biology and Medicine*; Pergamon Press: New York, 1983.

Scheme III

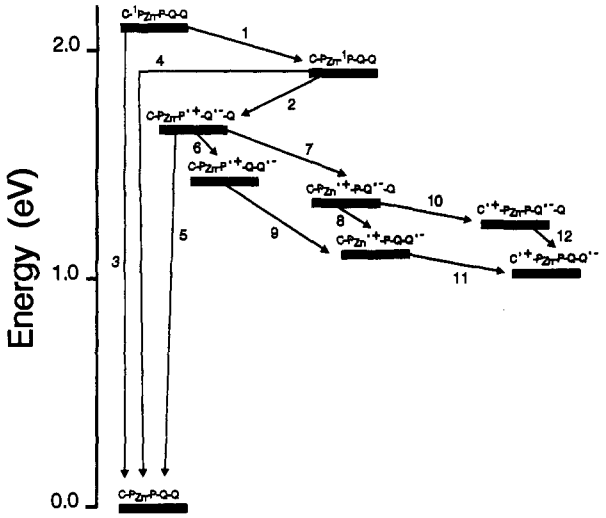

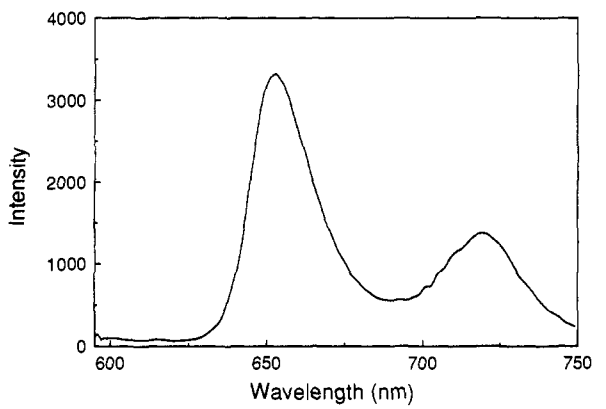

Figure 5. Steady-state fluorescence emission spectrum of pentad **2** in chloroform solution with excitation at 590 nm.

with charge recombination of the various charge-separated states shown in Scheme II. Step 5 is likely to be the main contributor to this recombination, as the positive and negative charges are in closest proximity in this species. Thus, the overall efficiency of charge separation could be enhanced by increasing the rate of step 6 and/or 7. Zinc-containing pentad **2** was designed to investigate this strategy. Insertion of the zinc ion results in stabilization of the porphyrin radical cation by 0.21 eV and, therefore, a comparable increase in the thermodynamic driving force for step 7 (Scheme III). Although the structure of **2** is identical to that of **1** with the exception of the metalation of one of the porphyrin moieties, the synthetic route to **2** differed significantly from that to **1** as a result of the necessity of ensuring that zinc was present in only the desired porphyrin macrocycle (see the supplementary material).

The absorption spectrum of **2** in dichloromethane is similar to that of **1**, with the exception that the free base porphyrin bands are reduced in relative amplitude and the typical zinc porphyrin absorptions appear at 592 and 550 nm. The Soret absorption appears as a single maximum at 422 nm.

Fluorescence studies were carried out in both dichloromethane and chloroform solutions. In both solvents, the emission spectra were similar to those observed for the free base porphyrins of **6**, **9**, and **1**, with maxima at 655 and 720 nm (Figure 5). Excitation at wavelengths where absorption was due mainly to the zinc porphyrin resulted in an additional very weak emission band at 611 nm, which is ascribed to that porphyrin. The emission from the free base porphyrin is quenched, relative to that from **8**, as was the case for **9** and **1**. The emission from the zinc porphyrin was quenched much more strongly, which is consistent with rapid singlet–singlet energy transfer from the zinc porphyrin to the free base, as has been observed in related porphyrin dyads.[13]

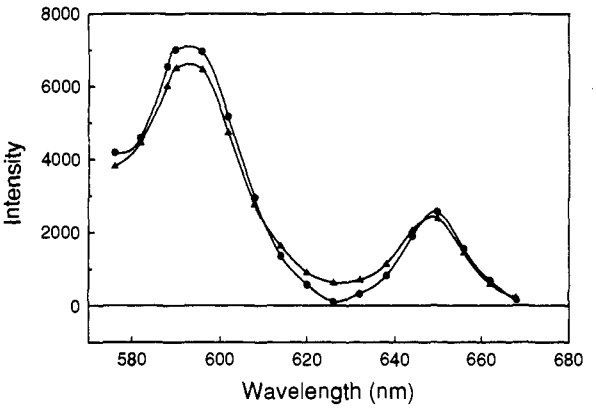

Figure 6. Absorption (●) and fluorescence excitation spectrum for 720-nm emission (▲) for pentad **2** in chloroform solution. The excitation spectrum has been corrected for the wavelength response of the excitation source and monochromator and normalized to the absorption spectrum in the 650-nm band, where all absorption is due to the free base porphyrin moiety. The emission at 720 nm is due mainly to the free base porphyrin.

The possibility of singlet–singlet energy transfer was investigated by obtaining the fluorescence excitation spectrum of **2** in chloroform solution. The corrected excitation spectrum for emission in the 720-nm region, where fluorescence is due essentially entirely to the free base porphyrin, was normalized to the absorption spectrum at 650 nm, where absorption is due only to that moiety. The results in the 580-670-nm region, where absorption from the carotenoid polyene is minimal, are shown in Figure 6. The excitation spectrum is nearly coincident with the absorption spectrum, demonstrating that the quantum yield of singlet–singlet energy transfer from the zinc porphyrin to the free base (step 1 in Scheme III) is very high.

Time resolved fluorescence emission data were obtained for **2** in both chloroform and dichloromethane. The results for a chloroform solution with 590-nm excitation appear in Figure 7. The data at the 14 wavelengths were analyzed globally as four exponential components ($\chi^2 = 1.12$). The two major components had lifetimes of 0.039 and 1.2 ns. Excitation at 650 nm, where only the free base porphyrin absorbs, yielded decay-associated spectra featuring the 1.2-ns decay, but lacking the 39-ps component.

The 39-ps component is associated with the decay of C-$^1P_{Zn}$-P-Q_A-Q_B, mainly by singlet–singlet energy transfer to the free base porphyrin. The positive contribution of this component to the decay-associated spectrum in the 600-nm region, where only the zinc porphyrin emits, and its negative amplitude in the 720-nm region (growth of fluorescence intensity following excitation) are consistent with the rise in population of C-P_{Zn}-^{1}P-Q_A-Q_B as C-$^1P_{Zn}$-P-Q_A-Q_B decays. The rate constant for singlet–singlet transfer (k_1 in Scheme III) may be estimated from eq 3, where τ_f is the 0.039-ns lifetime of C-$^1P_{Zn}$-P-Q_A-Q_B and k_3 is estimated as the reciprocal of the 0.37-ns fluorescence lifetime of carotenoporphyrin model **12** in chloroform. Thus, k_1 equals 2.3×10^{10} s^{-1}. The quantum yield for singlet transfer, given by (0.039×10^{-9}) k_1, is 0.90, which is consistent with the fluorescence excitation results discussed above, within experimental error.

$$1/\tau_f = k_1 + k_3 \qquad (3)$$

The presence of the diquinone moiety in **2** plays no role in the quenching of C-$^1P_{Zn}$-P-Q_A-Q_B. This is demonstrated by results for C-P_{Zn}-P triad **13** (Chart VI). Fluorescence decay studies of a ca. 1×10^{-5} M chloroform solution of **13** with 590-nm excitation were carried out at 10 wavelengths in the 625–745-nm region. Global analysis (Figure 8, $\chi^2 = 1.15$) yielded two major components with lifetimes of 0.039 and 7.2 ns. Virtually identical results were obtained in dichloromethane solution ($\chi^2 = 1.13$). The 0.039-ns component is reminiscent of that observed for **2** (Figure 7) and is associated with the decay of C-$^1P_{Zn}$-P. The

Chart VI

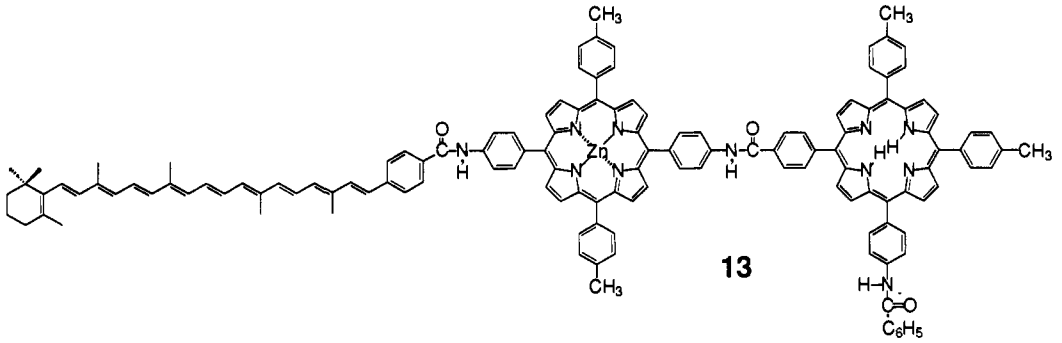

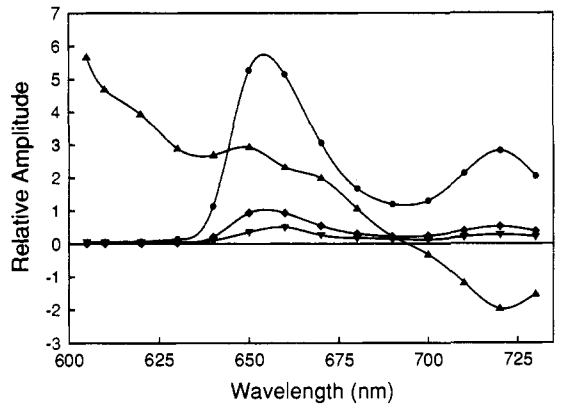

Figure 7. Decay-associated fluorescence emission spectrum for ca. 1 × 10^{-6} M pentad **2** in chloroform solution following excitation at 590 nm. The spectrum was obtained from a global analysis of data at the 14 indicated wavelengths (χ^2 = 1.12) analyzed as four exponentials with lifetimes of 0.039 (▲), 1.2 (●), 4.6 (◆), and 0.25 ns (▼).

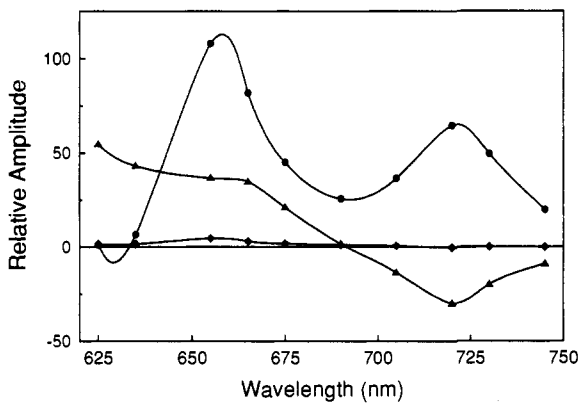

Figure 8. Decay-associated fluorescence emission spectrum for ca. 1 × 10^{-6} M triad **13** in chloroform solution following excitation at 590 nm. The spectrum was obtained from a global analysis of data at the 10 indicated wavelengths (χ^2 = 1.15) analyzed as three exponentials with lifetimes of 0.039 (▲), 7.2 (●), and 0.47 ns (◆).

quenching of the metalated porphyrin singlet state from the 0.37-nm lifetime observed for **12** is again ascribed to singlet–singlet energy transfer analogous to step 1 in Scheme III. Equation 3 yields a singlet–singlet energy-transfer rate constant of 2.3 × 10^{10} s^{-1} and a corresponding quantum yield of 0.90. The 7.2-ns component of the decay in Figure 8 has the shape of the free base porphyrin emission and is due to C-P_{Zn}-^{1}P. The lifetime is similar to those observed for **7** and **8**:[9] attachment of the zinc carotenoporphyrin moiety does not significantly affect the decay of the free base porphyrin first excited singlet state.

Turning now to the other major component of the fluorescence decay of pentad **2**, it is clear from the spectrum of the 1.2-ns emission that it is due to the free base porphyrin moiety. The short lifetime relative to that of **8** (7.8 ns in chloroform) and the free base porphyrin moiety of **13** is consistent with the quenching of the steady-state fluorescence intensity mentioned earlier and is attributed to electron transfer via step 2 in Scheme III. The rate constant for this photoinitiated electron transfer may be estimated as

$$k_2 = (1/\tau_f) - (1/\tau_0) \quad (4)$$

where τ_f is 1.2 ns and τ_0 is the 7.8-ns fluorescence lifetime of **8**. Thus, k_2 equals 7.1 × 10^8 s^{-1}. The corresponding quantum yield, based on C-P_{Zn}-^{1}P-Q_A-Q_B, is $k_2 \times \tau_f$, or 0.85.

Similar decay-associated spectra were obtained for **2** in dichloromethane. Global analysis of decays at 13 wavelengths in the 600–720-nm region with excitation at 590 nm yielded two major and two minor components with spectral shapes similar to those in Figure 7. From these data, the lifetime of C-$^1P_{Zn}$-P-Q_A-Q_B was found to be 0.035 ns, whereas that of C-P_{Zn}-^{1}P-Q_A-Q_B was 2.46 ns. The fluorescence lifetime of **12** in dichloromethane was 0.31 ns. If one assumes that the quenching of the zinc porphyrin singlet state in dichloromethane is due to singlet transfer, as was the case in chloroform, eq 3 yields a value of 2.5 × 10^{10} s^{-1} for k_1, which is virtually identical to that measured in chloroform and to that for singlet–singlet transfer in a structurally related porphyrin dyad in dichloromethane.[13] The quantum yield of singlet–singlet transfer is (0.035 × 10^{-9}) k_1, or 0.89. As was the case in chloroform, the quenching of the free base porphyrin first excited singlet state is associated with electron transfer by step 2 in Scheme III. The photoinduced electron transfer rate constant from eq 4 is 2.9 × 10^8 s^{-1}, and the corresponding quantum yield is 0.71.

Scheme III shows that C-P_{Zn}-$P^{\bullet+}$-$Q_A^{\bullet-}$-Q_B can in principle recombine via step 5 or evolve through steps 6 and 7 and subsequent electron transfers to yield $C^{\bullet+}$-P_{Zn}-P-Q_A-$Q_B^{\bullet-}$. Excitation of **2** in chloroform solution with a 650-nm laser pulse led to the formation of a long-lived transient absorption with a maximum at 970 nm, which was assigned to the carotenoid radical cation of the $C^{\bullet+}$-P_{Zn}-P-Q_A-$Q_B^{\bullet-}$ charge-separated state (Figure 9). An exponential fit of the decay with a floating base line yielded a lifetime for this species of 55 μs. As was the case with free base pentad **1**, there was a small amount of a very slowly decaying component that may represent intermolecular electron transfer to or from a neutral ground state or impurity. When examined on a shorter time scale, the decay shows a prompt rise to ~90% of its maximum intensity immediately (<5 ns) after excitation and reaches the peak value within several microseconds. The reason for the minor, slow component is presently unknown. Results for related molecules[13,15] suggest that it is not due to slow electron transfer by any of the steps in Scheme III, but rather to some relatively slow structural or environmental change in the molecule. The quantum yield of $C^{\bullet+}$-P_{Zn}-P-Q_A-$Q_B^{\bullet-}$ based on the maximum transient absorption is 0.83. Formation of a long-lived charge-separated state was also observed in dichloromethane following excitation at 650 nm. The lifetime of $C^{\bullet+}$-P_{Zn}-P-Q_A-$Q_B^{\bullet-}$, ~200 μs, was longer than that in chloroform, but the quantum yield was reduced to 0.60.

Pentad 3. The form of the pentad in which both porphyrin moieties are metalated was easily prepared by stirring a solution

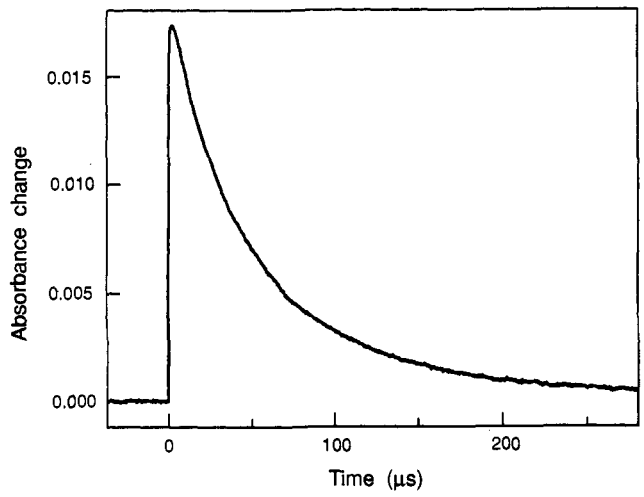

Figure 9. Decay of the transient absorbance at 970 nm of the $C^{\bullet+}$-P_{Zn}-P-Q_A-$Q_B^{\bullet-}$ state of pentad **2** following excitation of a ca. 5 × 10^{-6} M solution of **2** in chloroform with a 10-ns, 650-nm laser pulse. A three-parameter fit of these data as an exponential decay with a floating base line yields a lifetime of 55 μs.

Scheme IV

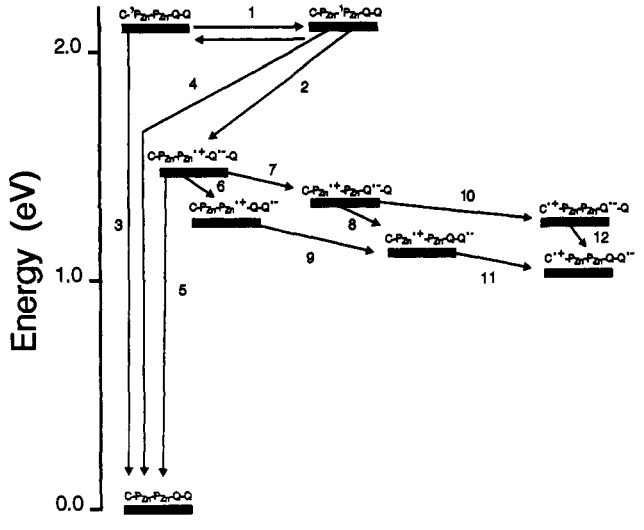

of **1** with an excess of zinc acetate and purifying the product. The absorption spectrum of **3** in dichloromethane features carotenoid and quinone bands similar to those observed for **1** and **2** and typical zinc porphyrin absorptions at 590, 548, and 424 nm. The emission spectrum is also typical of a zinc porphyrin, with maxima at 602 and 650 nm. Time resolved fluorescence emission studies were performed in dichloromethane with excitation at 590 nm. Global analysis of the decays at six wavelengths in the 610–670-nm region yielded a major component (amplitude ≥92% at all wavelengths) with a lifetime of 0.23 ns and a minor component of 0.54 ns (χ^2 = 1.24). The major component is consistent with rapid singlet–singlet energy transfer between the two porphyrin moieties, whose first excited singlet states are essentially isoenergetic at 2.07 eV, and decay of the two excited states by the usual routes (steps 3 and 4 in Scheme IV) and by electron transfer to the attached naphthoquinone via step 2. The electron-transfer rate constant k_2 is calculated to be 4.8 × 10^9 s^{-1}, using eq 1 and estimating k_4 as 6.8 × 10^8 s^{-1} from the 1.48-ns fluorescence lifetime of model porphyrin **14** in dichloromethane and k_3 from the lifetime for **12** in this solvent given above. The quantum yield of C-P_{Zn}-$P_{Zn}^{\bullet+}$-$Q_A^{\bullet-}$-Q_B, calculated according to eq 2, is 0.55.

Transient absorption studies of **3** in dichloromethane with 590-nm laser excitation showed that, as with the pentads discussed above, a long-lived charge-separated state, $C^{\bullet+}$-P_{Zn}-P_{Zn}-Q_A-$Q_B^{\bullet-}$, is formed. The quantum yield is 0.15, and the lifetime of the state is 120 μs.

Chart VII

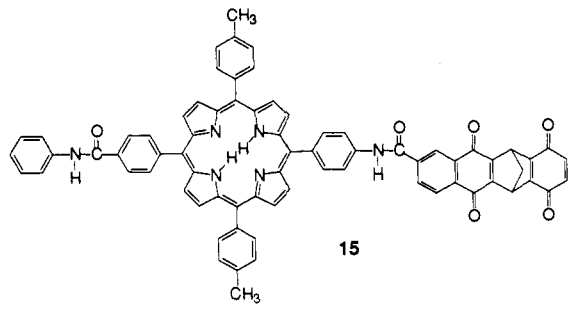

Pentads with Increased Porphyrin–Quinone Electronic Coupling. The results for pentads **1–3** show that, in all of these cases, the quantum yield is limited in part by the rate of photoinduced electron transfer step 2, which cannot compete with steps 3 and 4 to the extent necessary to achieve a quantum yield of unity. The photoinduced electron transfer step can be made much more rapid, and therefore more efficient, by increasing the electronic coupling between the porphyrin and naphthoquinone. A series of pentads and related molecules (**4**, **5**, **15**) (Chart VII) were prepared in order to investigate the effects of increased coupling. The structures of **4** and **5** are similar to that of **2**, with the exception that the porphyrin–diquinone linkage is reversed and the methylene spacer is removed. On the basis of studies of a C-P-Q_A-Q_B tetrad with a similar linkage,[15] photoinduced electron transfer from the free base porphyrin to the naphthoquinone in these molecules is expected to occur in less than 50 ps. The first reduction potentials of the naphtho- and benzoquinone moieties of the diquinone portions of **4**, **5**, and **15** (estimated from those[22] for model diquinone **16**) are identical within experimental error to those found for diquinone **10**. The first oxidation potential of a model for the free base porphyrin moiety of **4**, **5**, and **15** is lower by 0.07 eV than that for a comparable model for pentads **1** and **2**. These relatively small differences suggest that any differences in electron-transfer rates may be ascribed mainly to the alteration in electronic coupling between the porphyrin and quinone species.

P-Q_A-Q_B Triad 15. The absorption spectrum of the porphyrin moiety of **15** in chloroform is virtually identical to those of model porphyrins **7** and **8**. The emission spectrum is similar to that of **1** with maxima at 655 and 720 nm, and the emission is strongly quenched. Fluorescence decay studies were carried out on a ca. 1 × 10^{-5} M solution of **15** in chloroform with excitation at 590 nm. Decays were obtained at 11 wavelengths in the 630–745-nm region and analyzed globally as the sum of exponentials (χ^2 = 1.24) to yield a major component with a lifetime of 0.017 ns and three very minor contributors, which will be ignored. This short lifetime compared to the 7.8-ns lifetime of porphyrin **8** in chloroform is consistent with rapid electron transfer from the porphyrin moiety of ^{1}P-Q_A-Q_B to the attached quinone to produce the $P^{\bullet+}$-$Q_A^{\bullet-}$-Q_B charge-separated state. Application of eq 4 yields an electron-transfer rate constant of 5.9 × 10^{10} s^{-1}. The quantum yield of $P^{\bullet+}$-$Q_A^{\bullet-}$-Q_B is (5.9 × 10^{10})(0.017 × 10^{-9}), or 1.0.

Almost identical results were obtained for **15** in dichloromethane. Global analysis of fluorescence decays at 11 wavelengths in the 630–745-nm region following excitation at 590 nm yielded a fluorescence lifetime of 0.018 ns for ^{1}P-Q_A-Q_B, which in turn gives a rate constant for photoinduced electron transfer of 5.5 × 10^{10} s^{-1} and a quantum yield of 0.99.

Pentad 4. The results for **15** suggest that incorporation of the same porphyrin–quinone linkage into pentad **4** should lead to a very high yield for the initial photoinduced electron transfer. The steady-state emission spectrum of **4** is essentially identical in shape to that of pentad **2**. Fluorescence decay studies in chloroform were carried out initially with excitation at 650 nm,

(22) Gust, D.; Moore, T. A.; Moore, A. L.; Seely, G.; Liddell, P.; Barrett, D.; Harding, L. O.; Ma, X. C.; Lee, S.-J.; Gao, F. *Tetrahedron* **1989**, *45*, 4867–4891.

Scheme V

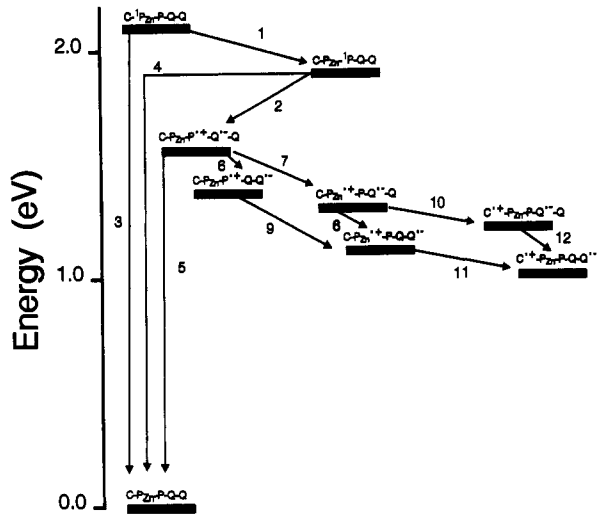

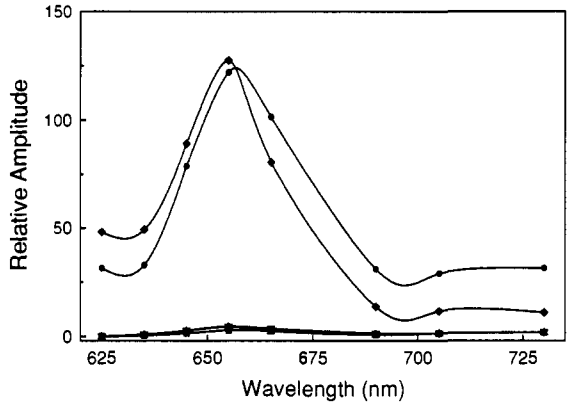

Figure 10. Decay-associated fluorescence emission spectrum for ca. 1×10^{-6} M pentad **4** in chloroform solution following excitation at 590 nm. The spectrum was obtained from a global analysis of data at the eight indicated wavelengths ($\chi^2 = 1.07$) analyzed as five exponentials with lifetimes of 0.018 (◆), 0.050 (●), 0.38 (▲), 1.8 (▼), and 6.4 ns (■).

where only the free base porphyrin moiety absorbs light. A total of 11 decays were measured in the 635–750-nm region. Global analysis yielded a major component with the emission spectrum of the free base porphyrin having a lifetime of 0.014 ns and three very minor contributions ($\chi^2 = 1.13$). Thus, the free base porphyrin first excited singlet state is strongly quenched. The results for model compounds **13** and **15** discussed above show that this quenching is due to electron transfer to the diquinone moiety (step 2 in Scheme V). Application of eq 4 using the results for **4** and **13** yields a value for k_2 of 7.1×10^{10} s^{-1} and a quantum yield of C-P_{Zn}-$P^{\bullet+}$-$Q_A^{\bullet-}$-Q_B equal to 0.99. Thus, these results are very similar to those obtained for model P-Q_A-Q_B molecule **15**.

Fluorescence decay studies were also carried out in chloroform with 590-nm excitation. In this case, the free base and metalated porphyrin moieties are both excited, and a mixture of C-P_{Zn}-^{1}P-Q_A-Q_B and C-$^1P_{Zn}$-P-Q_A-Q_B is produced. Decays were measured at eight wavelengths and analyzed globally ($\chi^2 = 1.07$) as the sum of five exponential processes (Figure 10). The two significant decays had lifetimes of 0.018 and 0.050 ns. It will be noted from the figure that the decay-associated spectrum no longer features the growth of fluorescence in the 720-nm region, which was characteristic of energy transfer from the zinc porphyrin to the free base moiety in **2** and **13**. The reason for this is clear, based on a kinetic analysis which includes steps 1–4 in Scheme V. The results from 650-nm excitation of **4** establish that k_2 is 7.1×10^{10} s^{-1}. The model studies on compounds **12** and **13** mentioned above allow estimation of k_1, k_3, and k_4 as 2.3×10^{10}, 2.7×10^9, and 1.4×10^8 s^{-1}, respectively. If these values are applied to pentad **4**, then it is apparent that electron-transfer step 2 is the most rapid decay pathway in the system and, in particular, that it is faster than singlet–singlet energy transfer. Under these conditions, C-$^1P_{Zn}$-P-Q_A-Q_B is expected to decay exponentially with a lifetime of about 0.040 ns, as was observed for **2** and **13**. However, the kinetics for C-P_{Zn}-^{1}P-Q_A-Q_B are considerably more complex. Some of this species will be formed by direct excitation and will decay with a lifetime of 0.014 ns, as was observed with 650-nm excitation. However, additional C-P_{Zn}-^{1}P-Q_A-Q_B will be formed as a result of singlet–singlet energy transfer with a rate constant of about 2.3×10^{10} s^{-1}. Thus, although the lifetime of the C-P_{Zn}-^{1}P-Q_A-Q_B formed by direct excitation will be about 0.014 ns, the observed decay of the total C-P_{Zn}-^{1}P-Q_A-Q_B fluorescence will be nonexponential at first and will evolve to a "lifetime" of about 0.040 ns as it becomes controlled by the lifetime of its precursor, C-$^1P_{Zn}$-P-Q_A-Q_B. Thus, the fit of the fluorescence data to two lifetimes of 0.018 and 0.050 ns shown in Figure 10 is only an approximation to a more complicated kinetic process. However, these two lifetimes are similar enough to those measured in the model compounds and with 650-nm excitation that the values given above for k_1-k_4 can be taken to apply to **4** (Table I). The singlet–singlet energy-transfer rate constant k_1, estimated as 2.3×10^{10} s^{-1}, and the corresponding calculated quantum yield of 0.90 are in reasonable accord with steady-state fluorescence excitation studies of **4**, which give quantum yields of energy transfer of 0.81 and 0.84 in chloroform and dichloromethane, respectively.

In short, pentad **4** behaves as a combination of model C-P_{Zn}-P triad **13** and model P-Q_A-Q_B triad **15**. Linking the various moieties does not introduce any significant new decay pathways, nor does it materially affect the rates of the various energy- and electron-transfer process.

The fluorescence results show that excitation of either porphyrin moiety of **4** will produce a C-P_{Zn}-$P^{\bullet+}$-$Q_A^{\bullet-}$-Q_B charge-separated state within 50 ps of excitation. The quantum yield of this state is unity with 650-nm excitation and nearly 1 with excitation at 590 nm. Scheme V and the results for **1** and **2** suggest that this initial charge-separated state will either rapidly recombine to yield the ground state by step 5 or evolve via steps 6–12 to yield a final $C^{\bullet+}$-P_{Zn}-P-Q_A-$Q_B^{\bullet-}$ species. Excitation of a ca. 7×10^{-6} M solution of **4** in chloroform with a 10-ns laser pulse at 650 nm resulted in the observation of a transient carotenoid radical cation spectrum that is similar to those seen with **1** and **2** and is ascribed to the $C^{\bullet+}$-P_{Zn}-P-Q_A-$Q_B^{\bullet-}$ charge-separated state. The quantum yield was 0.28, and the lifetime of the state was 5.3 μs. With 590-nm excitation, the quantum yield dropped slightly to 0.22.

In dichloromethane solution with 590-nm excitation, pentad **4** yields time resolved fluorescence decay results virtually identical to those obtain in chloroform. Thus, within experimental error, the rate constants estimated above for chloroform solution also apply in dichloromethane. A final $C^{\bullet+}$-P_{Zn}-P-Q_A-$Q_B^{\bullet-}$ charge-separated state was again observed by transient absorption spectroscopy. The quantum yield was ~0.04 with either 650-nm or 590-nm excitation. The lifetime of the final state was 64 μs.

Pentad 5. This pentad is identical in structure of **4**, with the exception that the quinone experiences a 5,10 relationship with the metalated porphyrin, rather than the 5,15 relationship found in **1-4**. To a first approximation, this molecule would be expected to have rate constants for photoinduced energy and electron transfer processes which are virtually identical to those found for **4** if, as suggested by Scheme V, all of the significant transfers occur between directly linked moieties. Indeed, this is the case for the steps leading to formation of the final $C^{\bullet+}$-P_{Zn}-P-Q_A-Q_B-$^{\bullet-}$ state. A ca. 1×10^{-6} M solution of **5** in chloroform was excited at 590 nm, and fluorescence decays were measured at eight wavelengths in the 610–690-nm region. For the reasons discussed above, kinetic analysis of the resulting data in accord with Scheme V was not attempted. However, global analysis as five exponential decays ($\chi^2 = 1.13$) yielded a decay-associated spectrum similar

to Figure 10 featuring two major components with lifetimes of 0.005 and 0.045 ns. Similar studies in dichloromethane yielded lifetimes of 0.013 and 0.047 ns ($\chi^2 = 1.13$). Examination of data from many multiwavelength experiments showed that the results for **5** were indistinguishable from those for **4**, within experimental error. Thus, values for k_1, k_2, k_3, and k_4 of 2.3×10^{10}, 7.1×10^{10}, 2.7×10^9, and 1.4×10^8 s^{-1} are estimated for **5** in both solvents.

The formation of a final charge-separated state $C^{\bullet+}$-P_{Zn}-P-Q_A-$Q_B^{\bullet-}$ was studied using transient absorption spectroscopy. In chloroform solution, excitation of a 7×10^{-6} M solution of **5** with a laser pulse at either 650 or 590 nm led to the formation of $C^{\bullet+}$-P_{Zn}-P-Q_A-$Q_B^{\bullet-}$ with a quantum yield of 0.25 or 0.18, respectively, and a lifetime of only 0.42 μs. Similar experiments in dichloromethane gave a quantum yield of 0.05 and a lifetime of 46 μs. Thus, pentad **5** behaves in a manner essentially identical to isomer **4**, with the exception of the shorter lifetime for the final charge-separated state in chloroform solution.

The reduced quantum yields of $C^{\bullet+}$-P_{Zn}-P-Q_A-$Q_B^{\bullet-}$ observed for **4** and **5** with 590-nm excitation are due in part to the fact that singlet energy transfer from the zinc porphyrin to the free base occurs with an efficiency of only ~90%. As the reductions are greater than 10%, other factors must contribute as well. A reduction in quantum yield in **2** with 590-nm excitation was also observed.[12] The nature of these additional factors is as yet unknown.

Discussion

As the tetrad and pentad systems mentioned above are closely related structurally and mechanistically, comparison of the results for these molecules can help us elucidate some of the factors controlling the rates and quantum yields of the various electron-transfer steps. This is the case even though the results given above contain no direct observations of the rates and yields of the various electron-transfer events intervening between photoinduced electron transfer and formation of the final charge-separated states. It will be noted that, within this series of pentads, **2** in chloroform solution gave the highest quantum yield for the final $C^{\bullet+}$-P_{Zn}-P-Q_A-$Q_B^{\bullet-}$ state. A fruitful way to discuss the results is to compare the performance of the various pentads with that of **2** and to deduce reasons for any differences.

Pentad 2 in Dichloromethane: Effect of Solvent. When the solvent is changed from chloroform to dichloromethane, the quantum yield of $C^{\bullet+}$-P_{Zn}-P-Q_A-$Q_B^{\bullet-}$ in pentad **2** drops from 0.83 to 0.60. There are two reasons for this change. In the first place, the rate constant for photoinduced electron transfer step 2 (Scheme III) in dichloromethane is only about 0.4 times that in chloroform, and this reduces the quantum yield of the initial step from 0.85 to 0.71. Similar reductions in the rate of photoinduced electron transfer upon changing the solvent from chloroform to dichloromethane have been observed in porphyrin–quinone dyads.[23] Secondly, the change in solvent evidently affects the rates of dark reactions so that steps 6–12 in Scheme III are not able to compete as efficiently with charge recombination of the various intermediates.

Pentads 1 and 3: Effect of Metalation. Although removal of the zinc from pentad **2** does not significantly alter the rate of photoinduced electron transfer step 2 (Table I), it does result in a substantially lower quantum yield of the initial charge-separated state, C-P-$P^{\bullet+}$-$Q_A^{\bullet-}$-Q_B, in **1** (0.36). This is due in part to the fact that removal of the zinc renders C-^{1}P-P-Q_A-Q_B and C-P-^{1}P-Q_A-Q_B essentially isoenergetic, and this in turn results in rapid singlet–singlet energy transfer between the two porphyrin moieties (step 1 in Scheme II and its reverse). Although the decay pathways for C-P-^{1}P-Q_A-Q_B appear not to be directly affected by the carotenoid (see results for triad **13** and tetrad **9**), the lifetime of C-^{1}P-P-Q_A-Q_B is somewhat reduced by the attached carotene (see, for example, the results for **7** and **11**). This quenching is most likely electron or energy transfer between the porphyrin and carotenoid moieties.[24] Thus, when the two porphyrin first excited singlet states are rapidly exchanging singlet excitation, the quantum yield of C-P-$P^{\bullet+}$-$Q_A^{\bullet-}$-Q_B is reduced relative to that in **2**, because of the increased rate of decay of C-P-^{1}P-Q_A-Q_B via energy transfer to the porphyrin bearing the carotenoid followed by relaxation according to step 3.

The yield of the final $C^{\bullet+}$-P-P-Q_A-$Q_B^{\bullet-}$ state in **1** is further reduced from 0.36 to 0.15 in dichloromethane due to inefficient competition of steps 6–12 in Scheme II with charge recombination. As a first approximation, it is reasonable to postulate that step 5 is the most rapid charge recombination reaction, as the π-electron systems bearing the positive and negative charges are spatially and electronically most strongly coupled in the C-P_{Zn}-$P^{\bullet+}$-$Q_A^{\bullet-}$-Q_B state. Although the thermodynamic driving forces for steps 5 and 6 in Scheme II are expected to be essentially identical to those for the comparable steps in pentad **2** (Scheme III), the driving force for step 7 in free base pentad **1** (0.11 eV) is substantially reduced from that for this step in zinc pentad **2** (0.32 eV). As these reaction exergonicities are presumably in the normal region of Marcus theory for electron transfer,[25,26] step 7 is expected to be substantially slower in **1** than in **2**. This undoubtedly accounts for the decrease in efficiency of the dark reactions in **1**.

The dimetalated pentad **3** also has a reduced quantum yield for the final species, $C^{\bullet+}$-P_{Zn}-P_{Zn}-Q_A-$Q_B^{\bullet-}$, (0.15) relative to **2** (0.60) in dichloromethane. Again, two factors conspire to produce this result. The rate of photoinduced electron transfer step 2 for **3**, where the metalloporphyrin is the donor species, is about 17 times greater than that for **2**, where the free base porphyrin is the donor. This is due to the greater driving force for step 2 in the dimetalated pentad (~0.60 eV, Scheme IV), which in turn is the result of a higher-energy first excited singlet state and a more stable porphyrin radical cation. At first glance, this enhancement might be expected to result in a higher quantum yield for the initial charge-separated state C-P_{Zn}-$P_{Zn}^{\bullet+}$-$Q_A^{\bullet-}$-Q_B. This is not realized because the zinc porphyrin first excited singlet state C-P_{Zn}-$^1P_{Zn}$-Q_A-Q_B has a substantially shorter lifetime in the absence of electron transfer than does C-P_{Zn}-^{1}P-Q_A-Q_B and because this state rapidly exchanges singlet excitation with the adjacent porphyrin to give C-$^1P_{Zn}$-P_{Zn}-Q_A-Q_B, which is also short-lived (Table I). Thus, the quantum yield of C-P_{Zn}-$P_{Zn}^{\bullet+}$-$Q_A^{\bullet-}$-Q_B in **3** is only 0.55 in dichloromethane, whereas that of C-P_{Zn}-$P^{\bullet+}$–$Q_A^{\bullet-}$-Q_B in **2** is 0.71.

The yield of $C^{\bullet+}$-P_{Zn}-P_{Zn}-Q_A-$Q_B^{\bullet-}$ in **3** is further reduced by inefficient competition of steps 6–12 with charge recombination. This is likely due, for the most part, to the large decrease in driving force, and therefore rate, for step 7 in **3** relative to **2**, which results from metalation of both porphyrin moieties (cf. Schemes III and IV).

Pentads 4 and 5: Effect of Electronic Coupling. These two molecules are closely related, and the rate constants for energy transfer and charge separation are identical, within the limits of error of this study. With excitation at 650 nm, for example, the yields of the final $C^{\bullet+}$-P_{Zn}-P-Q_A-$Q_B^{\bullet-}$ states for these molecules are ~0.25 in chloroform and ~0.05 in dichloromethane. The reduction in quantum yield relative to **2** is not due to the photoinduced electron transfer step 2 (Scheme V) because this very rapid step occurs with a yield of essentially unity. Therefore, the reduction must result from inefficient competition with charge recombination. The rate constants for steps 6 and 7 are expected to be essentially identical for **2**, **4** and **5**, as these steps do not involve porphyrin–quinone electron transfer, and the changes in the porphyrin–quinone linkage have only a small effect on the thermodynamic driving force for these reactions. However, the

(23) Schmidt, J. A.; Siemiarczuk, A.; Weedon, A. C.; Bolton, J. R. *J. Am. Chem. Soc.* **1985**, *107*, 6112–6114.

(24) Hermant, R. M.; Liddell, P. A.; Lin, S.; Alden, R. G.; Kang, H. K.; Moore, A. L.; Moore, T. A.; Gust, D. *J. Am. Chem. Soc.* **1993**, *115*, 2080–2081.

(25) Marcus, R. A. *J. Chem. Phys.* **1956**, *24*, 966–978.

(26) Marcus, R. A. *Annu. Rev. Phys. Chem.* **1964**, *15*, 155–196.

electronic coupling between the porphyrin and diquinone moieties has been greatly increased in pentads **4** and **5**, relative to **1–3**, and this increase evidently increases the rate of charge recombination by step 5, as well as that of step 2. The net result is that competition of steps 6 and 7 with charge recombination is not very efficient, especially in dichloromethane.

Lifetimes of the Final Charge-Separated States. The mechanism of charge recombination of the final $C^{\bullet+}$-P_{Zn}-P-Q_A-$Q_B^{\bullet-}$ state in **2** and related states in the other pentads has not been addressed in detail by this study. However, some conclusions can be drawn. The energies of these final states in all five pentads are expected to be essentially identical under any given set of conditions. Also, pentads **1–3** have identical linkages between the various moieties, and therefore molecular conformations and internuclear distances (e.g., benzoquinone–carotenoid separations and orientations) are not expected to differ strongly within this set of molecules. However, the lifetime of the final charge-separated state in dichloromethane varies significantly among the three compounds. In particular, successive introduction of zinc ions into the porphyrin moieties leads to shortening of the lifetimes (Table I). This result suggests that charge recombination may involve the porphyrin moieties, even though they are not ionic centers. They could take part through superexchange (through-bond) coupling of the carotenoid radical cation and the benzoquinone radical anion, or via endergonic population of some of the intermediate charge-separated states in the schemes followed by charge recombination. For example, the enhanced stabilization of a positive charge on the porphyrin macrocycle resulting from metalation would facilitate migration of the hole from the carotenoid toward the diquinone moiety.

The lifetime of the final state of pentad **4** is substantially shorter than that for the corresponding state of **2** under comparable conditions. This result is consistent with the change in porphyrin–quinone linkage, which both brings the carotenoid and benzoquinone moieties spatially closer together and increases the electronic coupling between the porphyrin and diquinone species.

Although the $C^{\bullet+}$-P_{Zn}-P-Q_A-$Q_B^{\bullet-}$ states of **4** and **5** have comparable lifetimes in dichloromethane, the lifetime in chloroform for **5**, which features the 5,10 linkage of the metalated porphyrin and diquinone moieties to the free base porphyrin, is more than 10 times shorter than that for **4**, with the 5,15 linkage. This short lifetime may result from the ability of **5** to assume conformations in chloroform in which atomic centers on the benzoquinone and metalated porphyrin approach one another to a separation of <4 Å. Molecular mechanics calculations of the type discussed earlier show that this is possible even if one considers only changes in dihedral angle resulting from rotations about single bonds. Such conformations may be sampled more frequently in chloroform than dichloromethane. These conformations are precluded in the molecules featuring the 5,15 linkage.

Conclusions

These studies allow one to draw several conclusions concerning the construction of artifical photosynthetic reaction centers. In the first place, excitation of pentad **2** in chloroform solution leads to the formation of a $C^{\bullet+}$-P_{Zn}-P-Q_A-$Q_B^{\bullet-}$ charge-separated state with a quantum yield approaching unity which has a long lifetime and preserves about half of the original excitation energy as chemical potential. These results are not unlike those found for natural bacterial reaction centers. Thus, although a great deal remains to be learned about various aspects of the natural process, it is now possible to mimic its general features in artificial systems which lack a protein component.

Secondly, it will be noted that pentads such as **2** achieve a high level of discrimination against charge recombination reactions by employing two multistep electron-transfer strategies. The first is sequential multistep electron transfer such as is observed in natural reaction centers. For example, the photoinduced electron transfer step 2 in pentad **2** yields C-P_{Zn}-$P^{\bullet+}$-$Q_A^{\bullet-}$-Q_B, which decays by sequential electron-transfer steps whose function is to move the positive charge to the carotenoid end of the molecule and the negative charge to the benzoquinone (e.g., steps 7, 10 and 12). The result is a charge-separated state which is long-lived, because of the large spatial separation of the charges, but which is formed in high quantum yield because each step in the sequence is fast relative to charge recombination and therefore efficient. The second is a parallel multistep electron-transfer strategy. For example, charge recombination step 5 in Scheme III is undoubtedly one of the most rapid charge recombinations because of the proximity of the charges in C-P_{Zn}-$P^{\bullet+}$-$Q_A^{\bullet-}$-Q_B. The pentad employs two electron-transfer steps, 6 and 7, operating in parallel to compete with this charge recombination. Using this strategy, a higher quantum yield of the final $C^{\bullet+}$-P_{Zn}-P-Q_A-$Q_B^{\bullet-}$ state can be achieved than would be possible for one step acting alone with an efficiency of less than unity. This strategy appears not be used in bacterial reaction centers, but could operate in a reaction center approaching true C_2 symmetry. Both of these strategies are amenable to application in many other sorts of electron- and energy-transfer systems and chemical reactions in general.

Finally, these results illustrate that although manipulation of individual electron- and energy-transfer rate constants in the pentads based on application of existing energy- and electron-transfer theories is relatively facile, structural or environmental changes which affect some rate constants invariably affect others. Thus, rational engineering of structures such as the pentads to increase quantum yields, lifetimes, stored energy, etc. requires a very detailed knowledge of all the effects of a given structural alteration.

Experimental Section

The ^{1}H NMR spectra were recorded on a Varian Gemini spectrometer at 300 MHz, a Bruker AM-400 spectrometer at 400 MHz, or a Varian Unity spectrometer at 500 MHz. Unless otherwise specified, samples were dissolved in deuteriochloroform with tetramethylsilane as an internal reference. The numbering system for resonance assignments has been previously reported.[19] Mass spectra were obtained at 70 eV on a Varian MAT 311 mass spectrometer operating in EI mode, a Kratos MS 50 mass spectrometer operating at 8 eV in FAB mode, or a VESTEC spectrometer. Ultraviolet–visible spectra were measured on a Shimadzu UV2100U UV–vis spectrometer. Cyclic voltammetric measurements were carried out with either a PAR Model 173 potentiostat/galvanostat or a Pine Instrument Co. Model AFRDE4 potentiostat. All electrochemical measurements were performed in 1,2-dichloroethane or dichloromethane at ambient temperatures with a platinum-button working electrode, a silver-wire quasireference electrode, and a platinum-wire counter electrode. The electrolyte was 0.1 M tetra-*n*-butylammonium hexafluorophosphate, and ferrocene was included as an internal reference redox system.

Fluorescence decay measurements were performed on $<1 \times 10^{-5}$ M solutions in air-saturated dichloromethane or chloroform at room temperature by the time-correlated single-photon counting method. All samples were purified either by column chromatography or by TLC prior to use. The solvents were distilled and stored over anhydrous potassium carbonate to remove any hydrochloric acid present. The excitation source was a frequency-doubled Coherent Antares 76s Nd:YAG laser routed through a variable beam splitter to pump a cavity-dumped dye laser.[27] The instrument response function was measured at the excitation wavelength (590 or 650 nm) for each decay experiment with a Ludox AS-40 under the same conditions as the sample. Nanosecond transient absorption measurements were carried out on $\sim 1 \times 10^{-5}$ M solutions in air-saturated dichloromethane or chloroform with excitation at 590 nm. The apparatus has been described elsewhere.[28] For each sample, absorption spectra were obtained before and after the experiment to rule out degradation of the compound. The yields of the final charge-separated states were determined by the comparative method,[21] as reported previously[10] using the triplet state of *meso*-tetratolylporphyrin as a reference.

(27) Gust, D.; Moore, T. A.; Luttrull, D. K.; Seely, G. R.; Bittersmann, E.; Bensasson, R. V.; Rougée, M.; Land, E. J.; De Schryver, F. C.; Van der Auweraer, M. *Photochem. Photobiol.* **1990**, *51*, 419–426.

(28) Davis, F. S.; Nemeth, G. A.; Anjo, D. M.; Makings, L. R.; Gust, D.; Moore, T. A. *Rev. Sci. Instrum.* **1987**, *58*, 1629–1631.

Detailed descriptions of the synthesis of the compounds mentioned in the text and their precursors are given in the supplementary material.

Acknowledgment. This work was supported by a grant from the Division of Chemical Sciences, Office of Basic Energy Sciences, Office of Energy Research, U.S. Department of Energy (grant DE-FG0287ER13791). This is publication 174 from the Arizona State University Center for the Study of Early Events in Photosynthesis. The Center is funded by U.S. Department of Energy Grant DE-FG02-88ER13969 as part of the USDA/DOE/NSF Plant Science Center program.

Supplementary Material Available: Text giving synthesis and characterization of the molecules discussed in the text and their precursors (33 pages). Ordering information is given on any current masthead page.